

Article

Pollution Characteristics and Sources of Ambient Air Dustfall in Urban Area of Beijing

Yin Zhou ^{1,2}, Beibei Li ^{2,*}, Yuhu Huang ^{2,*}, Yu Zhao ^{2,3}, Hongling Yang ² and Jianping Qin ²

¹ Key Laboratory of Beijing on Regional Air Pollution Control, Beijing University of Technology, Beijing 100124, China; daisy123@emails.bjut.edu.cn

² National Engineering Research Center of Urban Environmental Pollution Control, Beijing Municipal Research Institute of Eco-Environmental Protection, Beijing 100037, China

³ Department of Environmental Engineering, Beijing Institute of Petrochemical Technology, Beijing 102627, China

* Correspondence: libeibei@cee.cn (B.L.); huangyuhu@cee.cn (Y.H.)

Abstract: Since 2016, the Ministry of Ecology and Environment and the Beijing Municipal Government have adjusted the minimum concentration limit for ambient air dustfall several times, indicating that they attach great importance to dustfall. To grasp the pollution characteristics and sources of dustfall, in this work, the filtration method was used to determine the insoluble dustfall and water-soluble dustfall in the urban area of Beijing. From our analysis, the influence of the meteorological parameters on dustfall was found, and the chemical components of dustfall were determined. The positive matrix factorization (PMF) model was also utilized to analyze the sources of dustfall. The results indicated that the average amount of dustfall in 2021–2022 was $4.4 \text{ t} \cdot (\text{km}^2 \cdot 30 \text{ d})^{-1}$, and the proportion of insoluble dustfall deposition was 82.4%. Dustfall was positively correlated with the average wind speed and temperature and negatively correlated with the relative humidity and rain precipitation. The impact of the meteorological parameters on insoluble dustfall and water-soluble dustfall was the opposite. The average proportions of crustal material, ions, organic matter, element carbon, trace elements, and unknown components were 48%, 16%, 14%, 1.4%, 0.20%, and 20%, respectively. The proportions of the crustal material and ions were the highest in spring (57%) and summer (37%). The contribution rates of fugitive dust source, secondary inorganic source, mobile source, coal combustion source, snow melting agent source, and other sources were 42.4%, 19.3%, 8.3%, 3.0%, 2.7%, and 24.3%, respectively. This study supported dustfall pollution control by analysing the pollutant characteristics and sources of dustfall from the standpoint of total chemical components. In order to better control dustfall pollution, control measures and evaluation standards for fugitive dust pollution should be formulated.

Keywords: dustfall; meteorological parameter; chemical composition; source apportionment; urban area of Beijing



Citation: Zhou, Y.; Li, B.; Huang, Y.; Zhao, Y.; Yang, H.; Qin, J. Pollution Characteristics and Sources of Ambient Air Dustfall in Urban Area of Beijing. *Atmosphere* **2024**, *15*, 544. <https://doi.org/10.3390/atmos15050544>

Academic Editors: Honglei Wang, Lijuan Shen and Xugeng Cheng

Received: 20 March 2024

Revised: 16 April 2024

Accepted: 25 April 2024

Published: 29 April 2024



Copyright: © 2024 by the authors. Licensee MDPI, Basel, Switzerland. This article is an open access article distributed under the terms and conditions of the Creative Commons Attribution (CC BY) license (<https://creativecommons.org/licenses/by/4.0/>).

1. Introduction

In 1994, the former State Environmental Protection Bureau first issued the China environmental protection industry standard named the “Gravimetric method for the determination of dustfall in ambient air” [1], where dustfall refers to the particles that naturally settle in the dust collection container due to gravity under the conditions of the air environment [1]. In December 2021, the Ministry of Ecology and Environment revised and issued the “Gravimetric Method for Determination of Dustfall in Ambient Air”, for which the standard number is HJ 1221—2021 [2]. China’s Environmental Status Bulletin announced that the annual average dustfall in China from 1995 to 1997 was $16.4 \text{ t} \cdot (\text{km}^2 \cdot 30 \text{ d})^{-1}$ [3], and Wang et al. [4] reported that the annual mean dustfall in China from 1991 to 2011 was $14.7 \text{ t} \cdot (\text{km}^2 \cdot 30 \text{ d})^{-1}$. In another interesting work, Liu et al. pointed out that the average amount of dustfall in China from 2010 to 2019 was $8.4 \text{ t} \cdot (\text{km}^2 \cdot 30 \text{ d})^{-1}$; this amount was

about 43% lower than that from 1991 to 2011 [5]. In recent years, the former Ministry of Environmental Protection emphasized the accurate assessment of dustfall. In parallel, the “Beijing–Tianjin–Hebei Air Pollution Prevention and Control Measures (2016–2017)” proposed for the first time using “the average dustfall of $9 \text{ t}\cdot(\text{km}^2\cdot 30 \text{ d})^{-1}$ as the dustfall index” [6]. The average dustfall in Beijing in 2020 was $5.7 \text{ t}\cdot(\text{km}^2\cdot 30 \text{ d})^{-1}$, which is lower than that in other northern Chinese cities such as Xi’an, Lanzhou, Taiyuan, and Shijiazhuang [7–9]. However, dustfall pollution in Beijing is still worse than in southern Chinese cities. More specifically, the average dustfall in Beijing in 2020 was 1.1 times that of Nanchang in Jiangxi Province in 2015, 1.5 times that of Nanjing in Jiangsu Province in 2019, and 2.1 times that of Shenzhen in Guangdong Province in 2016 [10–12]. The gap between Beijing and cities in developed countries was even wider: the average dustfall in Beijing in 2020 was 3.6 times that of Colorado in the United States in 2017, 6.3 times that of Sydney in Australia in 2008, 7.6 times that of the Canary Islands in Spain in 2012, and 11.4 times that of Salkes in France in 2012 [12–16]. Compared with cities in southern China and developed countries, Beijing has a larger population. As a result, the number of people being affected by dustfall pollution is huge.

Various chemical component and source analyses on dustfall have been carried out in the literature by using $\text{PM}_{2.5}$ -based research methods [17–19]. Among the diverse pollutants, the heavy metal pollution characteristics of dustfall have been extensively studied [20–27], followed by the ion pollution characteristics and source analysis [28–32], but there are also a few works on persistent organic pollutants in dustfall [33–36]. Nevertheless, the characteristics and source analysis of total chemical components in dustfall have scarcely been examined [37,38].

In 2020, the dustfall in Dongcheng district and Xicheng district in Beijing was $4.7 \text{ t}\cdot(\text{km}^2\cdot 30 \text{ d})^{-1}$ and $5.3 \text{ t}\cdot(\text{km}^2\cdot 30 \text{ d})^{-1}$, respectively, ranked 5th and 10th among the 16 districts [39]. However, as the most densely populated area in Beijing, it is more vulnerable to the impact of dustfall pollution. Therefore, it is important to carry out a systematic study of the pollution characteristics and sources of dustfall in Beijing. Along these lines, in this work, the urban area of Beijing was selected as the research area, and the dustfall was chosen as the research object to thoroughly investigate the one-year pollution characteristics and sources of dustfall. The insoluble and water-soluble dustfall samples were obtained by using the filtration method of the American dustfall measurement standard [40]. The composition of insoluble and water-soluble dustfall in the dustfall was analyzed, and the impacts of monthly, seasonal, and meteorological parameters on the dustfall, as well as the amount of insoluble and water-soluble dustfall, were studied. In addition, the elements and carbonaceous components of insoluble dustfall, as well as the anions and cations of water-soluble dustfall, were determined. The composition characteristics of all chemical components in the dustfall and the source of the dustfall were systematically analyzed. Our work provides valuable technical support for the prevention and control of dustfall pollution in Beijing.

2. Materials and Methods

2.1. Study Area and Sampling

Beijing (115.7° – 117.4° E and 39.4° – 41.6° N) is located on the North China Plain and has a temperate monsoon climate, where spring and autumn are short, summer is hot and rainy, and winter is cold and dry. Xicheng district, which is located in the urban area of Beijing, was taken as the research area. It is densely populated, and human activities are complicated, which intensifies the impact of dustfall pollution in the Xicheng district. The monitoring point was set on the roof of a scientific research institution (116.355° N, 39.929° E), and the dustfall collection tank was 8 m above the ground, which meets the point setting requirements of HJ 1221–2021. There is a main road 60 m to the south of the monitoring site, and a secondary road 30 m to the east. The monitoring period was from June 2021 to June 2022 for a total of one year. In September 2021, no dustfall samples were collected due to the short-term construction of the roof.

2.2. Materials and Instruments

Dustfall collection containers and glycol solutions, as specified in HJ 1221–2021, were used to collect dustfall. The cylindrical dustfall collection tank with an inner diameter of 15 cm and a height of 30 cm was used, and the upper edge of the dustfall collection tank was 1.5 m from the roof surface. Moreover, metal screens with a 1 mm aperture [2,40], sand core filters, and filter membranes (mixed fiber and quartz filters) were utilized to filter the dustfall sample and obtain insoluble and water-soluble dustfall [41]. The dustfall samples collected from dustfall collection containers were filtered through the filter membrane under the pumping action of the sand core filter (Figure 1), and the dustfall was trapped on the filter membrane. Evaporators, ovens, dryers, and electronic balance were used to determine the amount of insoluble dustfall.

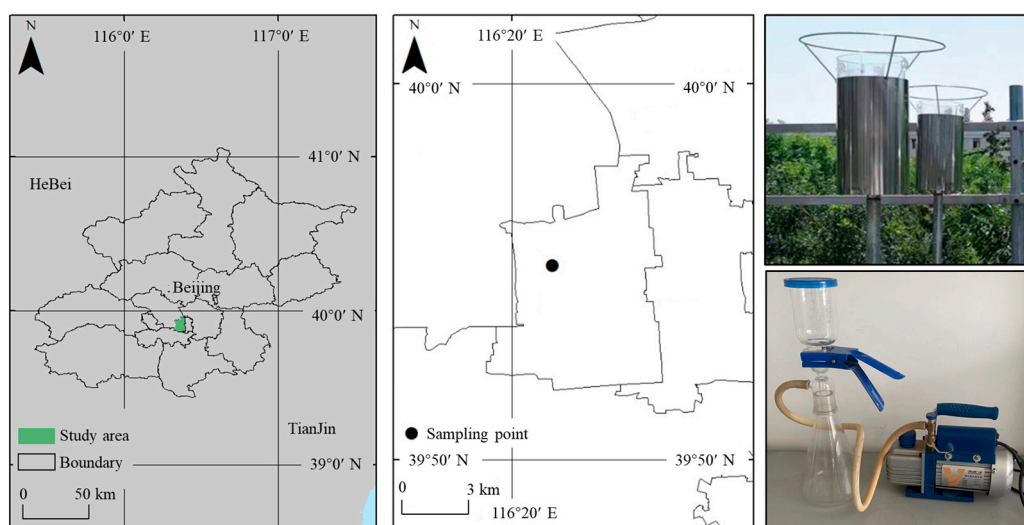


Figure 1. Location of the sampling point, dustfall collection containers, and sand core filter used in this research.

In this work, ion deposition was used to represent the water-soluble dustfall, and the total of other components except the water-soluble dustfall represented the insoluble dustfall. The insoluble dustfall included elemental oxides, elemental carbon (EC), and organic matter (OM). According to HJ 657–2013 [42], inductively coupled plasma mass spectrometry (ICP-MS) measurements were performed to determine the elements (i.e., Li, Be, V, Cr, Mn, Co, Ni, Cu, Zn, As, Se, Sr, Mo, Ag, Cd, Sn, Sb, Ba, Tl, Pb, Bi, Th, U, Al, Fe) of insoluble dustfall filtered using a mixed cellulose filter membrane. The elements of insoluble dustfall from mixed cellulose filter membranes were determined as a supplement to the results extracted via the ICP-MS method. EC and OC from the quartz filter membrane were determined by using a DRI2001A thermos-optical organic carbon/elemental carbon analyzer. The ion determination (i.e., Na^+ , K^+ , Mg^{2+} , Ca^{2+} , NH_4^+ , F^- , Cl^- , NO_3^- , SO_4^{2-}) of water-soluble dustfall from the filter membrane was carried out by using an ion chromatograph (IC) according to HJ 799–2016 and HJ 800–2016 [43,44].

2.3. Research Method

In accordance with HJ 1221–2021, parallel samples of two dust collecting containers were placed. To obtain more dustfall samples for data analysis, dustfall sampling was conducted weekly, and sampling was conducted at 10:00 am every Monday. According to the American dustfall measurement standard [40] and the test procedure of Zhao et al. [32], insoluble and soluble dustfall samples were obtained, wherein the dustfall sample of one dust collecting container was filtered using a mixed cellulose filter membrane, and the other sample was a filtered using a quartz filter membrane.

First, the parallelism of the insoluble dustfall amount obtained using the two filtration membranes was compared to provide a basis for the chemical mass reconstruction of dustfall. Second, Beijing meteorological Station No. 54511 is a national basic meteorological station, which provides meteorological information on behalf of the Beijing region to participate in global exchange. The meteorological data of Beijing meteorological station No. 54511 during the monitoring period were collected to analyze the impact of month, season, and meteorological parameters on the dustfall. The meteorological data obtained in this work include wind speed, temperature, relative humidity, and rain precipitation. Third, the composition characteristics of all chemical components in dustfall were examined, and the positive matrix factorization (PMF) receptor model was used to explore the source of dustfall [45,46].

2.4. Chemical Mass Reconstruction of Dustfall

The chemical components of the dustfall, including crustal material elements, trace elements, ions, organic carbon (OC), and elemental carbon (EC), were determined in this work. The crustal elements include Al, Si, Ca, Fe, and Ti. ICP-MS measurements can determine the element component, but due to the limitation of the filter membrane material in this study, ICP-MS measurements can only determine the Al and Fe elements in five crustal elements. The $\rho(\text{Si})/\rho(\text{Al}) = 7.27$, $\rho(\text{Ca})/\rho(\text{Al}) = 5.02$, and $\rho(\text{Ti})/\rho(\text{Al}) = 0.0329$ were determined by the work of Li [47] in the analysis of the pollution characteristics and component sources of dustfall in Jinan city and used to estimate the concentrations of Si, Ca, and Ti. Taking into account the reconstruction method of PM_{2.5} chemical component mass [48], the chemical component mass of dustfall was reconstructed according to the following formula:

$$\rho(\text{dustfall}) = \rho(\text{OM}) + \rho(\text{EC}) + \rho(\text{FS}) + \rho(\text{trace element}) + \rho(\text{unknown component}) + \rho(\text{water-soluble ion}) \quad (1)$$

$$\rho(\text{OM}) = 1.4\rho(\text{OC}) \quad (2)$$

$$\rho(\text{FS}) = 2.2\rho(\text{Al}) + 2.49\rho(\text{Si}) + 1.63\rho(\text{Ca}) + 2.42\rho(\text{Fe}) + 1.94\rho(\text{Ti}) \quad (3)$$

In the formula, FS denotes crustal material.

2.5. PMF Modeling

Sources contributions to dustfall were determined using the US Environmental Protection Agency's (EPA) PMF. The PMF model offers the advantage of not necessitating a source spectrum, emission inventory, and pollutant photochemical reaction mechanism. In addition, it does not require high time consistency of sample data. By examining the internal correlation within the observed data, the PMF model analyzed the primary contributing factors and their respective magnitudes in accordance with local conditions, subsequently determining the types of sources represented by these factors based on the eigenvalues of different components across various factors. In this study, the US EPA PMF 5.0 was used to perform a multisite PMF analysis [22,45,46,49,50]. With a two-dimensional solution, a matrix of sample data could be decomposed into the factor contribution matrix G ($n \times p$) and factor profile matrix F ($p \times m$), in which p is the number of factors contributing to the samples. The conventional factor analysis-based method assumes that the initial data set X is denoted as in Equation (4):

$$X_{ij} = \sum_{k=1}^p g_{ik}f_{kj} + e_{ij} \quad (4)$$

where X is the concentration of species, I is the numbering of samples, j is the chemical species, f is the source profile, g is the mass contribution, and e is the residual for each sample and species. The number of sources (p) is a user-defined value. The model found the optimum solution based on the objective function (minimizing Q):

$$Q = \sum_{I=1}^n \sum_{j=1}^m \left(\frac{e_{ij}}{u_{ij}} \right)^2 \quad (5)$$

where u is the uncertainty of samples and species, and the uncertainties were calculated by

$$\text{If } X_{ij} \leq \text{MDL}, u_{ij} = \frac{5}{6} \times \text{MDL} \quad (6)$$

$$\text{If } X_{ij} \geq \text{MDL}, u_{ij} = \sqrt{(\sigma_j \times X_{ij})^2 + (\text{MDL})^2} \quad (7)$$

where σ_j is the relative standard deviation, and MDL is the minimum detection limit. For quality control purposes, samples and species inputs were pre-screened based on three criteria: volatility, the signal to noise (S/N) ratio, and the number of measurements missing.

3. Results and Discussion

3.1. Time Variation Characteristics of Dustfall

Figure 2 shows the parallelism results of the insoluble dustfall measurement. As can be seen, the linear regression equation of insoluble dustfall measured using the quartz filter and mixed cellulose filter membranes is $y = 1.01x - 0.06$ and $R^2 = 0.97$, respectively, which is highly correlated. This result indicates that both filter membranes can be used to determine insoluble dustfall and can be combined to extract the chemical components of insoluble dustfall.

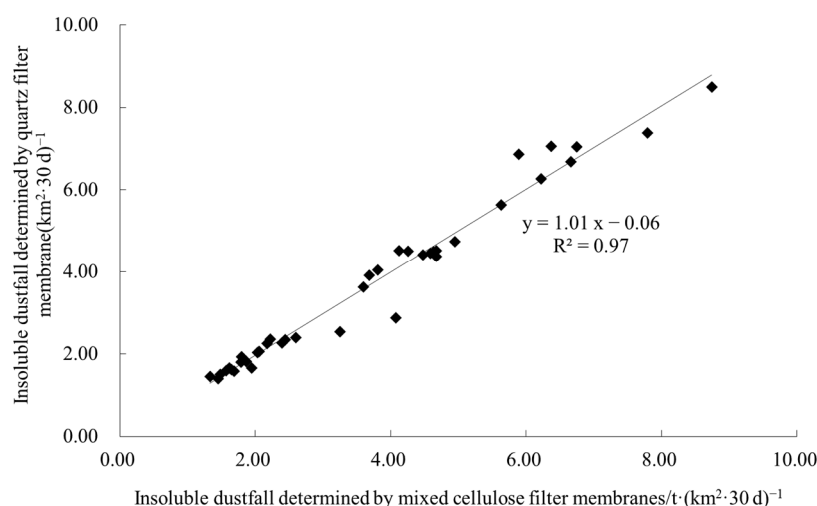


Figure 2. Parallelism of the determination results of insoluble dustfall.

Figure 3 depicts the monthly and quarterly dustfall in 2021–2022. The annual average dustfall during the whole monitoring period was $4.4 \text{ t} \cdot (\text{km}^2 \cdot 30 \text{ d})^{-1}$, which is 12% lower than that in 2020. Compared with other cities in Table 1, the air quality of cities in northern China during the monitoring period was better, and the dustfall during the monitoring period was 0.52 times that of Taiyuan in Shanxi Province, 0.54 times that of Tianjin Province, and 0.55 times that of Shijiazhuang in Hebei Province [9,51]. However, there is still a gap between the urban area of Beijing and the southern cities. The dustfall during the monitoring period was 1.1 times that of Nanjing in Jiangsu Province and 1.6 times that of Shenzhen in Guangdong Province [12,13]. The dustfall in the core area was slightly higher than that in Mentougou district in 2021 ($4.3 \text{ t} \cdot \text{km}^{-2} \cdot 30 \text{ d}^{-1}$) and Tongzhou district in 2020 ($3.4 \text{ t} \cdot \text{km}^{-2} \cdot 30 \text{ d}^{-1}$), indicating that the dustfall pollution in the urban area of Beijing was more serious than that in the suburbs [52,53].

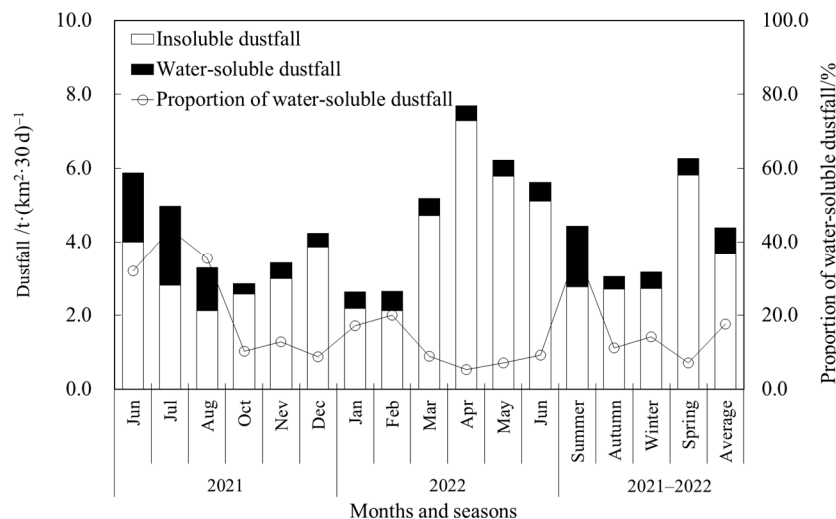


Figure 3. Monthly and seasonal dustfall from 2021 to 2022. Ion deposition was used to represent the water-soluble dustfall, and the total sum of other components except the water-soluble dustfall represents the insoluble dustfall.

Table 1. Dustfall/ $t \cdot (km^2 \cdot 30 d)^{-1}$ of typical cities in China.

Location	Typical City	Province	Sampling Period	Dustfall
North China	Taiyuan	Shanxi	2019.11–2020.12	8.5
	Tianjin	Tianjin	2020.01–12	8.1
	Shijiazhuang	Hebei	2020.01–12	8.0
	Beijing	Beijing	2018.01–12	7.5
	Beijing	Beijing	2019.01–12	5.6
	Beijing	Beijing	2020.01–12	5.0
	Beijing (this research)	Beijing	2021.06–2022.06	4.4
South China	Nanjing	Jiangsu	2019.01–12	3.9
	Shenzhen	Guangdong	2016.01–12	2.7

Table 2 presents the dustfall of foreign cities. Compared with typical cities in Europe, Oceania, and North America, the dustfall in Beijing was still high. The dustfall in the monitoring period was 8.8 times that of Salkes in France, 5.9 times that of the Canary Islands in Spain, 4.9 times that of Sydney in Australia, and 2.8 times that of Colorado in the United States [13–16]. Compared with African cities, the dustfall in the urban area of Beijing was low, being 0.50 times that of Tizi Ouzou in Algeria and 0.63 times that of Sfax in Tunisia [54,55]. Compared with typical Asian cities, the dustfall in Beijing was in the middle, being higher than Selangor in Malaysia and lower than Tabriz in Iran [14,18].

Table 2. Dustfall/ $t \cdot (km^2 \cdot 30 d)^{-1}$ of typical foreign cities.

Location	Typical City	Sampling Period	Dustfall
Europe	Salkes, France	2011.8–2012.12	0.5 ± 0.01
	The Canary Islands, Spain	2009–2012	0.75 ± 0.09
Oceania	Sydney, Australia	2007.6–2008.7	0.9
North America	Colorado, USA	2017.11–2018.11	1.58 ± 0.01
Africa	Tizi Ouzou, Algeria	2011.5–2012.12	5.5 ± 0.1
	Sfax, Tunisia	2012.11–2013.4	7
Asia	Selangor, Malaysia	2010.7–2010.10	3.9 ± 2.1
	Tabriz, Iran	2017.4–9	7.4 ± 5.6
	Beijing, China (this research)	2021.06–2022.06	4.4

The annual average of insoluble dustfall was $3.68 \text{ t}\cdot(\text{km}^2\cdot30 \text{ d})^{-1}$, and the annual average water-soluble dustfall was $0.71 \text{ t}\cdot(\text{km}^2\cdot30 \text{ d})^{-1}$. The proportion of insoluble dustfall in Beijing was $82.4\% \pm 13.7\%$, and the proportion of insoluble dustfall in the southeast of Spain from 2011 to 2013 was $44\% \pm 11\%$ [56], which is about twice that of Spain, indicating the higher impact of fugitive dust in Beijing. On top of that, the proportion of water-soluble dustfall in Beijing was 17.6%, of which the proportion of water-soluble dustfall in the winter and spring of 2021–2022 (from December of the first year to March of the next year) was 14.5%. This is similar to the proportion of water-soluble dustfall in the winter and spring of 2020–2021 (14.2%) [32], both of which are lower than the annual average (17.6%). This result is related to the low rainfall in autumn and winter.

From 2021 to 2022, the monthly dustfall and insoluble dustfall exhibited a double-peak and double-valley pattern, with two valley values appearing in January and October, and two peaks appearing in April and December. In April, the construction site resumes work, and in December, a large number of trees lose leaves, coupled with the heating season. Furthermore, the average windspeeds in April and December were 1.9 m/s and 1.6 m/s, so the wind speed is relatively high in these two months. Wind speed is considered an important factor affecting dustfall [29]. The water-soluble dustfall from 2021 to 2022 presents a unimodal pattern, with the peak appearing in summer, which is related to the concentration of annual precipitation in summer. Spring dustfall, spring insoluble dustfall, and spring water-soluble dustfall were 1.41, 2.05, and 1.98; 2.10, 2.14, and 2.14; and 0.27, 1.31, and 0.99 times those of summer, autumn, and winter, respectively. The seasonal variation in dustfall amount, insoluble dustfall amount, and water-soluble dustfall amount was different, which points out that the influence of meteorological parameters on the three dustfall amounts should be further analyzed.

3.2. Influence of Meteorological Parameters on Dustfall

Figure 4 displays the temporal changes in the meteorological parameters and weekly dustfall from 2021 to 2022. The following is a detailed analysis of the influence of meteorological parameters (precipitation, temperature, average wind speed, and relative humidity) on dustfall.

The Spearman correlation coefficient (ρ) between various dustfall and meteorological parameters is depicted in Table 3. As can be seen, the amount of dustfall was positively correlated with the average wind speed, weakly positively correlated with the temperature, weakly negatively correlated with relative humidity, and very weakly negatively correlated with precipitation [57,58].

Table 3. The Spearman correlation coefficient (ρ) between various dustfall/ $\text{t}\cdot(\text{km}^2\cdot30 \text{ d})^{-1}$ and meteorological parameters. (* indicated that the correlation was significant when the confidence level was 0.05; ** indicated that the correlation was significant when the confidence level was 0.01).

Types of Dustfall	Meteorological Parameters			
	Precipitation /mm	Temperature /°C	Average Wind Speed / $\text{m}\cdot\text{s}^{-1}$	Relative Humidity /%
Dustfall	−0.049	0.281	0.491 **	−0.274
Insoluble dustfall	−0.228	0.136	0.599 **	−0.427 **
Water-soluble dustfall	0.650 **	0.350 *	−0.367 *	0.551 **

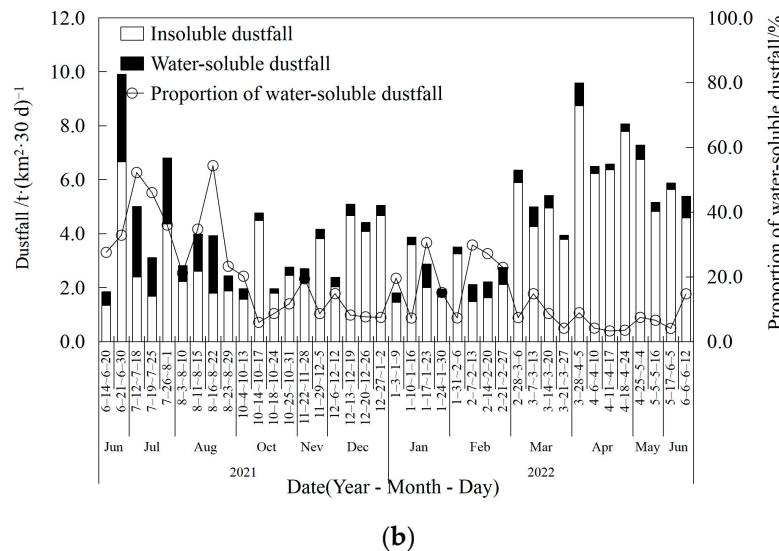
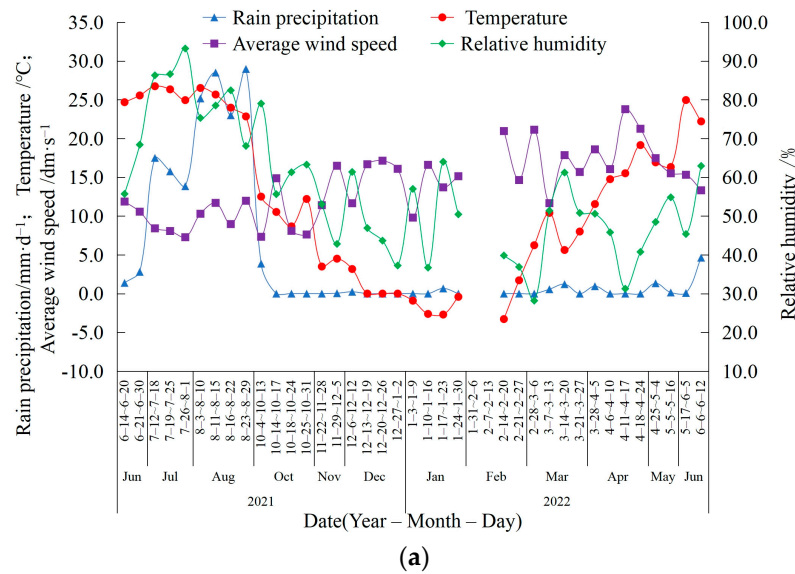


Figure 4. Temporal variations in meteorological parameters (a) and weekly dustfall (b) from 2021 to 2022.

To understand the connection between the dustfall and meteorological parameters, the relationship between insoluble and water-soluble dustfall and meteorological parameters was further analyzed, as shown in Table 3. The average wind speed had a positive correlation ($\rho = 0.599$) with insoluble dustfall and a moderate negative correlation ($\rho = -0.367$) with water-soluble dustfall. Moreover, the positive and negative partial cancellation made the dustfall have a moderate positive correlation with the average wind speed ($\rho = 0.491$). A very weak positive correlation between the temperature and insoluble dustfall ($\rho = 0.136$) and a weak positive correlation between the temperature and water-soluble dustfall ($\rho = 0.350$) were also observed. The weighted average of the two resulted in a weak correlation between dustfall and temperature ($\rho = 0.281$). The relative humidity was moderately negatively correlated with insoluble dustfall ($\rho = -0.427$) and moderately positively correlated with water-soluble dustfall ($\rho = 0.551$). The positive and negative partial cancellation caused a weak negative correlation between the dustfall and relative humidity ($\rho = -0.274$). Precipitation exhibited a weak negative correlation with insoluble dustfall ($\rho = -0.228$) and a strong positive correlation with water-soluble dustfall ($\rho = 0.650$), and the positive and negative partial cancellation meant that the dustfall had a very weak negative correlation with precipitation ($\rho = -0.049$). In summary, the correlation between

dustfall and the degree of moderate or lower meteorological parameters was because the meteorological parameters (except temperature) had completely opposite effects on insoluble and water-soluble dustfall. Considering the high proportion of insoluble dustfall in the dustfall in Beijing, it is suggested to pay attention to the prevention and control of dustfall pollution under weather conditions of high temperature and high wind speed.

3.3. Chemical Composition of Dustfall

Figure 5 displays the time variation in the chemical composition of dustfall from 2021 to 2022. The average proportions of crustal material, ions, OM, EC, trace elements, and unknown components during the whole sampling period from 2021 to 2022 were 48%, 16%, 14%, 1.4%, 0.20%, and 20%, respectively. In addition to the unknown components, the crustal material accounted for the highest proportion, followed by ions and OM, and the proportion of them was similar. On the contrary, EC and trace elements accounted for a relatively small proportion, which showed that the prevention and control of fugitive dust pollution is the primary task of controlling the dustfall pollution, while controlling the source of ions and OM is also very necessary. Compared with the dustfall components in Mentougou district from 2018 to 2022, the proportion of crustal material in this study is higher than that in Mentougou district (25.5%), and the proportion of OM and EC is lower than that in Mentougou district (20.6% and 2.3%). The crustal material is mainly from soil wind–sand dust and construction cement dust. OM and EC mainly come from combustion emissions such as gas-fired power plants, biomass burning, and waste incineration. This indicates that the core area of Beijing is more affected by fugitive dust than by combustion emissions [53,54].

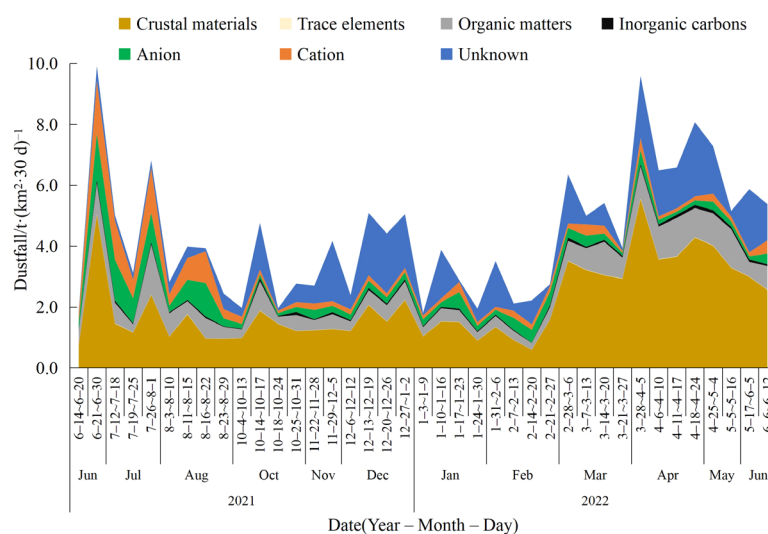


Figure 5. Temporal variation in chemical composition in dustfall from 2021 to 2022. The chemical substances contained in the composition are provided in Table S1 of the Supplementary Material.

Figure 6 shows the chemical compositions of dustfall corresponding to different seasons, dustfalls, and average wind speeds. From the perspective of the chemical composition of dustfall in different seasons, the proportion of crustal material in spring was the highest (57%). The proportions of crustal material in summer, autumn, and winter were 39%, 44%, and 43%, respectively. Ions occupied the highest proportion (37%) in summer and the lowest proportion (7.1%) in spring, whereas in autumn and winter, the proportions were 11% and 14%, respectively. In winter and spring (from December of the current year to March of the next year), the proportions of anions and cations were 60.0% and 40.0%, respectively, which is similar to the results of winter and spring in 2020–2021 [32]. NH_4^+ and K^+ were the main species of cations, accounting for 37% and 44%, respectively. SO_4^{2-} , NO_3^- , and Cl^- were the main species of anions, accounting for 51%, 25%, and 23%, respectively. SO_4^{2-} , NO_3^- , and NH_4^+ were important components of secondary aerosols, which are formed by

the secondary transformation of precursor SO_2 , NO_x , and NH_3 . K^+ and Cl^- usually come from the combustion process, and the proportions of K and Cl in ionic components in the dustfall from December 2021 to March 2022 in this study (19%) were higher than that in the same period last year (12%), indicating that the emission of combustion products in the Beijing core area had an increasing trend [32]. OM was lowest in winter (12%), 15% in spring, 16% in summer, and 15% in autumn. The proportion of unknown components was the lowest in summer (6.5%) and greater than 20% in other seasons, which may be related to the high precipitation in summer and the small average particle size of dustfall. According to the chemical compositions of different dustfall amounts, larger dustfall amounts lead to a bigger proportion of crustal material and a smaller proportion of OM. A smaller amount of dustfall indicates a larger proportion of ions. From the chemical composition of dustfall corresponding to different average wind speeds, a greater average wind speed suggests that the proportions of crustal materials and unknown components are also bigger. On the contrary, a lower average wind speed induces a larger proportion of ions and OM.

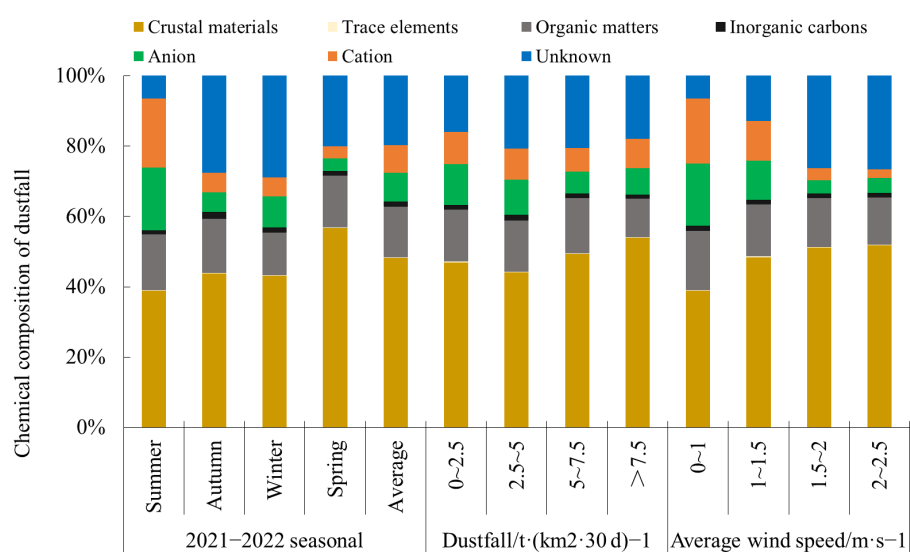


Figure 6. Chemical compositions of dustfall for different seasons, dustfall precipitation rates, and average wind speeds from 2021 to 2022.

3.4. Analysis of the Source of Dustfall

The amounts and uncertainty levels of 39 chemical components in the dustfall obtained during the sampling period were input into the PMF receptor model [44], and analysis of 5~7 factors was attempted during the calculation process of the PMF receptor model. The results showed that when the simulation output six factors, the eigenvalues and source spectra of each factor had distinct source indications, and each of them was independent. Figure 7 depicts the composition spectrum of the sources of dustfall pollution. In factor 1, OM and EC are the main components of the mobile source, with contribution rates of 50.7% and 46.3%, respectively, and can be regarded as the identifying components of the mobile source. NH_4^+ and SO_4^{2-} are the main components in factor 2, with contribution rates of 61.3% and 38.7%, respectively, which can be identified as secondary inorganic sources. In factor 3, the contents of Na^+ and Cl^- were high, and their contribution rates were 66.7% and 36.5%, respectively. Snow melting agent is used in Beijing snowfall, so it can be identified as the source of the snow melting agent source. In factor 4, the characteristic values of K^+ , SO_4^{2-} , and OM were high, and their contribution rates were 89.8%, 26.8%, and 53.2%, respectively. Therefore, this factor can be judged as the coal combustion source. In factor 5, although the contribution rate of F^- was 36.7%, there was no obvious corresponding identification source. Hence, it can be classified in the other source category. In factor 6, the contribution rates of Ca^{2+} , Mg^{2+} , Al, Si, and Fe were high, and their contribution rates

were 26.8%, 32.1%, 63.7%, 62.5%, and 61.8%, respectively. Thus, factor 6 can be identified as the fugitive dust source.

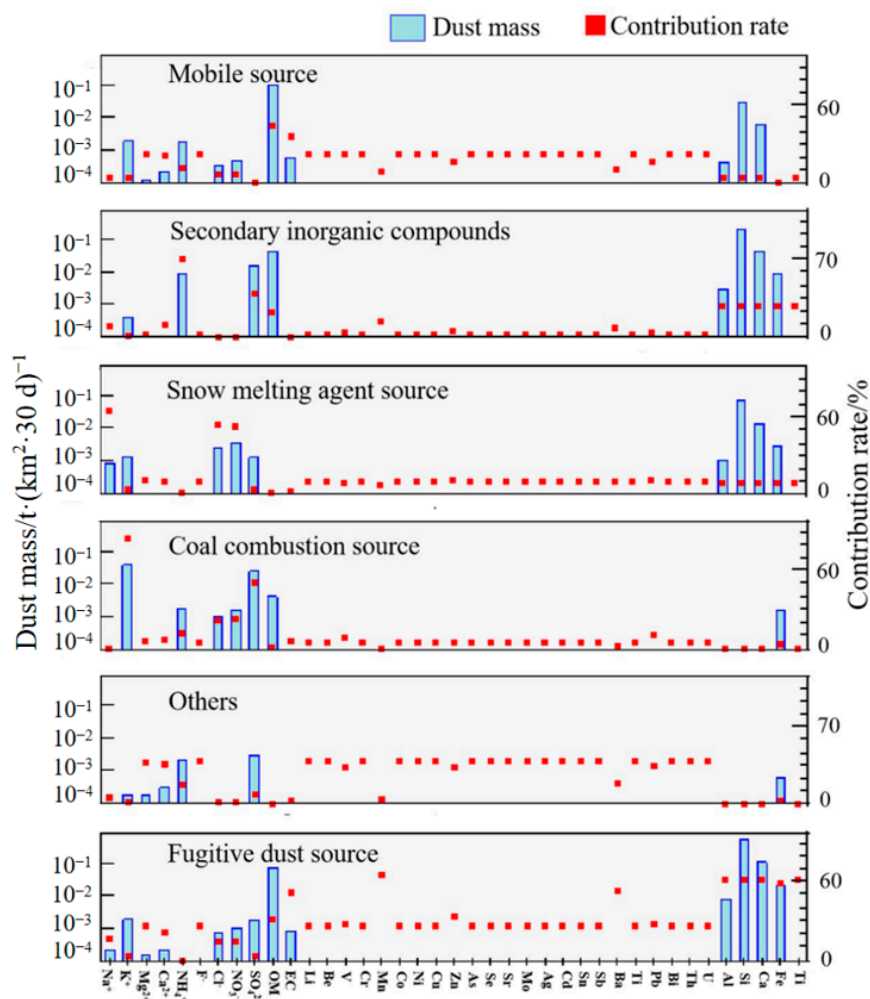


Figure 7. Composition profiles of the various dustfall pollution sources.

Figure 8 illustrates the contributions of dustfall pollution sources based on the PMF receptor model. As can be seen, the annual dustfall pollution sources in the urban area of Beijing include fugitive dust sources, secondary inorganic sources, mobile sources, coal combustion sources, snow melting agent sources, and other sources (including unknown components). The fugitive dust source is the most important source, with a contribution rate of 42.4%, which is more consistent with the actual situation in Beijing; the second is the secondary inorganic source, whose contribution rate is 19.3%. Mobile and coal combustion sources contributed 8.3% and 3.0%, respectively. The contribution of the snow melting agent source was 2.7%, which may be related to several snowfalls such as heavy snow on 6 November 2021, light snow on 23 December, light snow on 21 January, light snow on 30 January, medium snow on 13 February, and medium snow on 18 March. Snow melting agent is typically applied to roads during or after snowfall to facilitate rapid snowmelt and prevent road freezing. Following water evaporation, the residual snow melting agent particles adhere to the road surface, are stirred by vehicle movement, and re-enter the atmosphere as a component of dustfall. The contribution rate of other sources (including unknown components) was 24.3%. Compared with Zhang et al.’s study in Taiyuan, Shanxi Province, the contribution rate of fugitive dust sources in this study was higher than that in Taiyuan (14%), while the significant contributions of mobile and coal combustion sources were lower than those in Taiyuan (29%, 35%) [52]. This effect is related to the strict emission standards of motor vehicles and the high degree of clean energy substitution in Beijing. For

these reasons, the contribution of fugitive dust sources to dustfall reduction in Beijing is more prominent. In the future, Beijing should pay more attention to the control of fugitive dust sources, implement the technical specification of vehicle-mounted monitoring and evaluation for suspended dust load on paved roads, formulate and implement technical specifications for urban fugitive dust pollution prevention and control, and implement emissions standard for construction fugitive dust. In spring, the supervision of construction dust and road dust should be strengthened. In snowy weather, snow melting agents should be used moderately; when a large amount of snow melting agent is needed, the snow melting agent should be pre-wet.

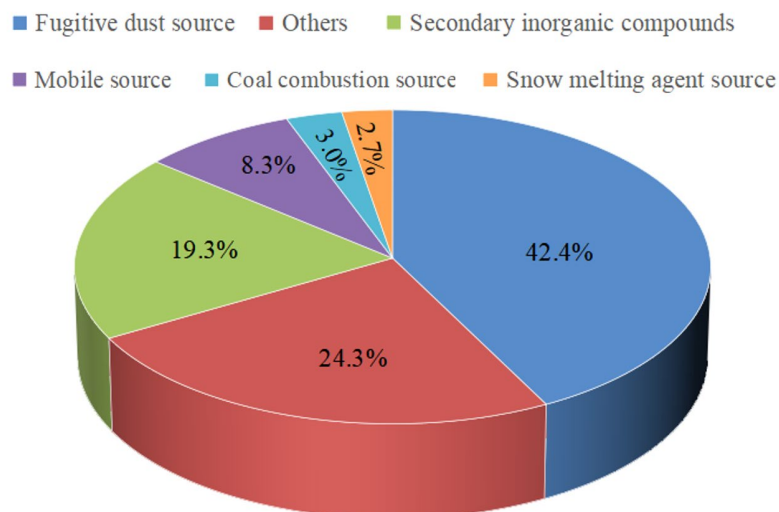


Figure 8. Composition profile of dustfall pollution sources.

4. Conclusions

To grasp the pollution characteristics and sources of dustfall, the filtration method was used to determine the insoluble dustfall and water-soluble dustfall in urban areas of Beijing. From our analysis, the influence of the meteorological parameters on dustfall was found, and the chemical components of dustfall were determined. The analysis of dustfall pollution characteristics and sources from total chemical components was carried out to provide support for dustfall pollution control.

Although the average amount of dustfall in 2021–2022 was $4.4 \text{ t} \cdot (\text{km}^2 \cdot 30 \text{ d})^{-1}$, which was better than cities in northern China, it had a significant gap compared with cities in southern China and typical cities in developed countries. The dustfall pollution in Beijing still needs to be further controlled. The proportion of insoluble dustfall was 82.4%, which indicated that dust has a significant impact on dustfall in Beijing. The monthly dustfall and insoluble dustfall showed double peaks and double valleys, and the water-soluble dustfall showed single peaks. The three peaks occurred in April, July, and December.

Dustfall was positively correlated with the average wind speed, weakly positively correlated with the temperature, weakly negatively correlated with relative humidity, and very weakly negatively correlated with precipitation. In addition, the Spearman correlation coefficients between dustfall and rain precipitation, relative humidity, temperature, and average wind speed were -0.049 , -0.274 , 0.281 , and 0.491 , respectively. The influences of meteorological parameters (except temperature) on the amount of insoluble dustfall and water-soluble dustfall were opposite, which could reflect the moderate and below-degree relationship of dustfall with each meteorological parameter.

The average proportions of crustal material, ions, OM, EC, trace elements, and unknown components were 48%, 16%, 14%, 1.4%, 0.20%, and 20%, respectively. The proportion of crustal material was highest in spring (57%), the proportion of ions was highest in summer (37%), and the proportion of OM was lowest in winter (12%). A larger amount of dustfall led to a bigger proportion of crustal material and a smaller proportion of OM.

In addition, a greater average wind speed induced a bigger proportion of crustal material and unknown components. Although the proportion of crustal material in the dustfall in Beijing city is the highest, it is still lower than that in Taiyuan City. The proportion of crustal materials is higher than that in Mentougou district, and the proportion of OM and EC is lower than that in Mentougou district, which indicates that the urban area of Beijing is more affected by fugitive dust. The proportions of K^+ and Cl^- in ionic components are higher than those in winter and spring of 2020–2021, indicating an increasing trend of combustion emissions. The proportion of unknown components is higher than that of $PM_{2.5}$, indicating that the chemical components of dustfall are more difficult to test.

The PMF model was used to analyze the source of dustfall in the urban area of Beijing in 2021–2022. The contribution rates of fugitive dust source, secondary inorganic source, mobile source, coal combustion source, snow melting agent source, and other sources (including unknown components) were 42.4%, 19.3%, 8.3%, 3.0%, 2.7%, and 24.3%, respectively. Compared with Taiyuan, Shanxi Province, the contribution of fugitive dust from the Beijing urban area is higher, and those from mobile sources and coal sources are lower. In the future, the Beijing urban area should pay attention to the control of fugitive dust sources and secondary inorganic sources and reduce the use of snow melting agents in winter.

In order to achieve accurate control of dustfall, future research directions should be combined with the changes in dustfall and particulate matter emission inventory in Beijing from 2018 to 2023, analyze the contribution ratios of various fugitive dust source pollution prevention measures in the three-year action plan to fight air pollution, ensure air pollution prevention, control action plans and other policies to ensure a decrease in dustfall, and carry out environmental and cost-benefit analyses of various measures.

Supplementary Materials: The following supporting information can be downloaded via this link: <https://www.mdpi.com/article/10.3390/atmos15050544/s1>, Table S1: Chemical substances contained in the composition.

Author Contributions: Conceptualization, Y.H.; methodology, B.L.; software, H.Y.; validation, Y.Z. (Yin Zhou), Y.H. and H.Y.; formal analysis, Y.Z. (Yin Zhou); investigation, Y.Z. (Yin Zhou), B.L., and J.Q.; resources, Y.H.; data curation, Y.Z. (Yu Zhao); writing—original draft preparation, Y.Z. (Yin Zhou); writing—review and editing, Y.H.; visualization, Y.Z. (Yin Zhou); supervision, Y.H.; project administration, B.L.; funding acquisition, Y.H. All authors have read and agreed to the published version of the manuscript.

Funding: This work was supported by the Finance Science and Technology Special Project of Beijing Xicheng District (grant number XCSTS-SD2020-02) and the Beijing Xicheng District Excellent Talents Training and Support Program (grant number XCRC-202031).

Institutional Review Board Statement: Not applicable.

Informed Consent Statement: Not applicable.

Data Availability Statement: The data presented in this study are available on request from the corresponding author. The data are not publicly available due to privacy.

Acknowledgments: We are grateful for meteorological data support from the China Meteorological Data Service Center (Beijing meteorological Station No. 54511).

Conflicts of Interest: The authors declare no conflicts of interest.

References

1. *GB/T 15265-94; Gravimetric Method for Determination of Dustfall in Ambient Air.* Ministry of Ecology and Environment of the People's Republic of China: Beijing, China, 1995.
2. *HJ 1221-2021; Gravimetric Method for Determination of Dustfall in Ambient Air.* Ministry of Ecology and Environment of the People's Republic of China: Beijing, China, 2022.
3. *Bulletin of China's Environmental Status over the Years;* Ministry of Ecology and Environment of the People's Republic of China: Beijing, China, 2020.

4. Wang, M.; Han, L.; Wang, M.; Cao, N.; Song, D. Study on the regional distribution of dustfall in China. *Ecol. Environ. Sci.* **2014**, *23*, 1933–1937.
5. Liu, L.Y.; Huang, Y.H.; Li, B.B.; Zhao, Y.; Qin, J.P. Research progress on sampling and determination methods of ambient air dustfall. *Environ. Sci. Technol.* **2021**, *44*, 104–112.
6. *Enhanced Measures to Prevent and Control Air Pollution in Beijing-Tianjin-Hebei Region (2016–2017) (Huanqi [2016] No. 80)*; Ministry of Environmental Protection of the People's Republic of China: Beijing, China, 2016.
7. Yang, W.; Chen, Y.; Zhao, J.; Hu, B. Spatial and temporal variation of atmospheric deposition pollution in Xi'an City. *Environ. Sci. Technol.* **2017**, *40*, 10–14.
8. Zhang, J.; Gao, H.; Wang, Y. Temporal and spatial variations of atmospheric dust-fall in Lanzhou. *Environ. Study Monit.* **2019**, *32*, 31–36.
9. *Dust Fall Monitoring Results of "2+26" Cities in the Beijing-Tianjin-Hebei Air Pollution Transmission Channel and 11 Cities in the Fenwei Plain in December 2020*; Ministry of Ecology and Environment of the People's Republic of China: Beijing, China, 2020.
10. Wei, B.; Zuo, J.; Wei, X. Analysis of dust fall in Nanchang, Jiangxi Province in 2015. *Sci. Technol. Innov.* **2016**, *11*, 97.
11. *2019 Nanjing Environmental Status Bulletin*; Nanjing Bureau of Ecological Environment: Nanjing, China, 2020.
12. *2016 Shenzhen Environmental Status Bulletin*; Shenzhen Bureau of Ecological Environment: Shenzhen, China, 2017.
13. Emeline, L.; Anna, A.; Malika, B.N.K.; Marie-Pierre, T. Atmospheric deposition of particulate matter between Algeria and France: Contribution of long and short-term sources. *Atmos. Environ.* **2018**, *191*, 181–193.
14. Patricia, L.G.; Maria, D.G.C.; Desire, S.C.; Miguel, S.; Cayetano, C.; Jose, J.H. A three-year time-series of dust deposition flux measurements in Gran Canaria, Spain: A comparison of wet and dry surface deposition samplers. *Atmos. Environ.* **2013**, *79*, 689–694.
15. Brett, S.D.; Gavin, F.B. Spatial distribution of bulk atmospheric deposition of heavy metals in metropolitan Sydney, Australia. *Water Air Soil Pollut.* **2011**, *214*, 147–162.
16. Heindel, R.C.; Putman, A.L.; Murphy, S.F.; Repert, D.; Hinckley, E. Atmospheric dust deposition varies by season and elevation in the Colorado front range, USA. *J. Geophys. Res. Earth Surf.* **2020**, *125*. [[CrossRef](#)]
17. Pura, M.; María, J.D.; Anthony, F.S.; Antonio, S. Spatial Identification and Hotspots of Ecological Risk from Heavy Metals in Urban Dust in the City of Cartagena, SE Spain. *Sustainability* **2023**, *16*, 307. [[CrossRef](#)]
18. Mehran, E.; Adeleh, Y.; Akbar, G. Temporal and spatial variations of deposition and elemental composition of dustfall and its source identification around Tabriz, Iran. *J. Environ. Health Sci. Eng.* **2019**, *17*, 29–40.
19. Li, Y.; Ma, L.; Ge, Y.; Abuduwaili, J. Health risk of heavy metal exposure from dustfall and source apportionment with the PCA-MLR model: A case study in the Ebinur Lake Basin, China. *Atmos. Environ.* **2022**, *272*, 118950. [[CrossRef](#)]
20. Li, C.; Wang, X.; Xiao, S.; Wang, H. The Source Apportionment of Heavy Metals in Surface Dust in the Main District Bus Stops of Tianshui City Based on the Positive Matrix Factorization Model and Geo-Statistics. *Atmosphere* **2023**, *14*, 591. [[CrossRef](#)]
21. Beauchemin, S.; Levesque, C.; Clare, L.S.W.; Rasmussen, P.E. Quantification and Characterization of Metals in Ultrafine Road Dust Particles. *Atmosphere* **2021**, *12*, 1564. [[CrossRef](#)]
22. Faisal, M.; Wu, Z.; Wang, H.; Hussian, Z.; Shen, C. Geochemical Mapping, Risk Assessment, and Source Identification of Heavy Metals in Road Dust Using Positive Matrix Factorization (PMF). *Atmosphere* **2021**, *12*, 614. [[CrossRef](#)]
23. Kabir, M.H.; Wang, Q.; Rashid, M.H.; Wang, W.; Isobe, Y. Assessment of Bioaccessibility and Health Risks of Toxic Metals in Roadside Dust of Dhaka City, Bangladesh. *Atmosphere* **2022**, *13*, 488. [[CrossRef](#)]
24. Shi, Z.; Lu, J.; Liu, T.; Zhao, X.; Liu, Y.; Mi, J.; Zhao, X. Risk assessment and source apportionment of available atmospheric heavy metal in a typical sandy area reservoir in Inner Mongolia, China. *Sci. Total Environ.* **2024**, *912*, 168960. [[CrossRef](#)] [[PubMed](#)]
25. Chen, L.; Zhou, S.; Tang, C.; Luo, G.; Wang, Z.; Lin, S.; Zhong, J.; Li, Z.; Wang, Y. A novel methodological framework for risk zonation and source-sink response concerning heavy-metal contamination in agroecosystems. *Sci. Total Environ.* **2023**, *868*, 161610. [[CrossRef](#)] [[PubMed](#)]
26. Cheng, Z.; Xu, S.; Na, X.; Zhang, X.; Ma, D.; Zhang, P. Spatial-Heterogeneity Analysis of the Heavy Metals Cd and Pb in Road Dust in the Main Urban Area of Harbin. *Sustainability* **2022**, *14*, 8007. [[CrossRef](#)]
27. Huang, W.; Wang, S.L. Distribution characteristics and sources of heavy metals in atmospheric deposition during heating and non-heating period in Lanzhou. *Environ. Sci.* **2022**, *43*, 597–607.
28. Qiu, L.; Qiao, J.; Ma, L.; Yang, Y. Research on the Effect of the Dustfall on the Statue Surface on the Water Migration of the Earthen Layer. *Asia Conf. Geol. Res. Environ. Technol.* **2021**, *632*, 022020. [[CrossRef](#)]
29. Li, Y.; Zhao, B.; Duan, K.; Cai, J.; Niu, W.; Dong, X. Assessments of Water-Soluble Inorganic Ions and Heavy Metals in Atmospheric Dustfall and Topsoil in Lanzhou, China. *Int. J. Environ. Res. Public Health* **2020**, *17*, 2970. [[CrossRef](#)] [[PubMed](#)]
30. Su, T.H.; Lin, C.S.; Liu, C.P. Dry deposition of particulate matter and its associated soluble ions on five broadleaved species in Taichung, central Taiwan. *Sci. Total Environ.* **2021**, *753*, 141788. [[CrossRef](#)] [[PubMed](#)]
31. Han, K.; Liu, R.H.; Xu, H.X.; Wang, Y.; Shao, L. Characteristics and sources of apportionment of water-soluble ion pollution in dustfall in Qingdao. *Environ. Eng.* **2022**, *40*, 111–117,193.

32. Zhao, Y.; Li, B.B.; Huang, Y.H.; Liang, J.; Yang, H.L.; Qin, J.P.; Zhu, L. Characteristics and Source Apportionment of Atmospheric Ion Deposition During Winter and Spring in the Core Area of Beijing. *Environ. Sci.* **2023**, *44*, 1865–1872.
33. Yun, J.; Zhang, Q.; Dou, M.; Wang, L. Characteristics, sources, bio-accessibility, and health risks of organophosphate esters in urban surface dust, soil, and dustfall in the arid city of Urumqi in China. *Sci. Total Environ.* **2024**, *912*, 169125. [[CrossRef](#)] [[PubMed](#)]
34. Liu, P.; Shao, L.; Li, Y.; Jones, T.; Cao, Y.; Yang, C.X.; Zhang, M.; Santosh, M.; Feng, X.; Bérubé, K. Microplastic atmospheric dustfall pollution in urban environment: Evidence from the types, distribution, and probable sources in Beijing, China. *Sci. Total Environ.* **2022**, *838*, 155989. [[CrossRef](#)] [[PubMed](#)]
35. Hishamuddin, N.H.; Khan, M.F.; Suradi, H.; Siraj, B.M.Z.; Islam, M.T.; Sairi, N.A.; Tajuddin, H.A.; Jamil, A.K.M.; Akanda, M.J.H.; Yusoff, S. The Sources of Polycyclic Aromatic Hydrocarbons in Road Dust and Their Potential Hazard. *Sustainability* **2023**, *15*, 12532. [[CrossRef](#)]
36. Liu, Y.; Mao, Y.; Xu, J.; Chen, W.; Xu, C.; Liu, W.; Qu, C.; Chen, W.; Zhang, J.; Xing, X.; et al. Health Risks Associated with Polycyclic Aromatic Hydrocarbons (PAHs) in Dustfall Collected from Universities in Wuhan, China. *Atmosphere* **2022**, *13*, 1707. [[CrossRef](#)]
37. Wang, H.J.; Song, C.; Cong, X.C. Chemical elemental analysis of dustfall particulate matter and identification of pollution sources at a harbour area. *Air Qual. Atmos. Health* **2024**, *10*, 1007. [[CrossRef](#)]
38. Tian, X.; Xie, Y.Q.; Xv, B.; Wei, Y.T.; Xv, H.; Zhang, Z.C.; Feng, Y.C.; Shi, G.L. Particle size characteristics of source apportionment and chemical composition of atmospheric dustfall in Taiyuan. *China Environ. Sci.* **2023**, *43*, 2755–2762.
39. *Monthly Report on Dustfall Control*; 12th issue of 2020; Beijing Municipal Bureau of Ecological Environment: Beijing, China, 2021.
40. ASTM D1739-98; Standard Test Method for Collection and Measurement of Dustfall. American Society of Testing Materials: West Conshohocken, PA, USA, 2017.
41. Laurent, B.; Losno, R.; Chevaillier, S.; Vincent, J.; Rouillet, P.; Bon Nguyen, E.; Ouboulmane, N.; Triquet, S.; Fournier, M.; Raimbault, P.; et al. An Automatic Collector to Monitor Insoluble Atmospheric Deposition: Application for Mineral Dust Deposition. *Atmos. Meas. Tech.* **2015**, *8*, 2801–2811. [[CrossRef](#)]
42. HJ 657-2013; Determination of Lead and Other Metallic Elements in Air and Exhaust Particulate Matter by Inductively Coupled Plasma Mass Spectrometry. Ministry of Ecology and Environment of the People's Republic of China: Beijing, China, 2013.
43. HJ 799-2016; Determination of Water-Soluble Anions (F^- , Cl^- , Br^- , NO_2^- , NO_3^- , PO_4^{3-} , SO_3^{2-} , SO_4^{2-}) in Ambient Air Particles by Ion Chromatography. Ministry of Ecology and Environment of the People's Republic of China: Beijing, China, 2016.
44. HJ 800-2016; Determination of Water-Soluble Cations (Li^+ , Na^+ , NH_4^+ , K^+ , Ca^{2+} , Mg^{2+}) in Ambient Air Particles by Ion Chromatography. Ministry of Ecology and Environment of the People's Republic of China: Beijing, China, 2016.
45. Nicolás, J.; Chiari, M.; Crespo, J.; Orellana, I.G.; Lucarelli, F.; Nava, S.; Pastor, C.; Yubero, E. Quantification of Saharan and local dust impact in an arid Mediterranean area by the positive matrix factorization (PMF) technique. *Atmos. Environ.* **2008**, *42*, 8872–8882. [[CrossRef](#)]
46. Xing, Z.Y.; Xiong, Y.; Du, K. Source apportionment of airborne particulate matters over the Athabasca oil sands region: Inter-comparison between PMF modeling and ground-based remote sensing. *Atmos. Environ.* **2020**, *221*, 117103. [[CrossRef](#)]
47. Li, S.L. *Characteristics and Source Analysis of Dust Pollution in Jinan City*; Shandong Jianzhu University: Jinan, China, 2019.
48. Huang, Y.; Li, M.; Qu, S.; Yan, J.; Pan, T. Characteristics of different components of PM_{2.5} light extinction coefficient in Beijing. *Res. Environ. Sci.* **2015**, *28*, 1193–1199.
49. Lu, Z.; Liu, Q.; Xiong, Y.; Huang, F.; Zhou, J.; Schauer, J.J. A hybrid source apportionment strategy using positive matrix factorization (PMF) and molecular marker chemical mass balance (MM-CMB) models. *Environ. Pollut.* **2018**, *238*, 39–51. [[CrossRef](#)]
50. Liu, B.; Yang, J.; Yuan, J.; Wang, J.; Dai, Q.; Li, T.; Bi, X.; Feng, Y.; Xiao, Z.; Zhang, Y.; et al. Source apportionment of atmospheric pollutants based on the online data by using PMF and ME2 models at a megacity, China. *Atmos. Res.* **2017**, *185*, 22–31. [[CrossRef](#)]
51. Zhang, Z.; Xie, T.; Zhang, Z.; Gao, G.; Xv, B.; Tian, X.; Xv, H.; Wei, Y.; Shi, G.; Feng, Y. Source analysis and seasonal variation characteristics of atmospheric dust fall in Taiyuan City based on two receptor models. *China Environ. Sci.* **2022**, *45*, 2577–2586.
52. Wang, Z.Y.; Yao, Q.; Lv, F.; Wang, Y.W.; Wang, S. Air dust pollution characteristics, chemical composition characteristics and quality reconstruction in Mentougou District, Beijing. *Environ. Sci.* **2023**, *44*, 6007–6014.
53. Lu, H.J.; Liu, B.X.; Shen, X.E.; An, X.X.; Ma, T.F.; Zhang, Z.; Liu, Z.Y. Study on the seasonal characteristics and measuring conditions of dustfall in Beijing area. *Environ. Prot. Sci.* **2022**, *48*, 125–128.
54. Bahloul, M.; Chabbi, I.; Sdiri, A.; Amdouni, R.; Medhioub, K.; Azri, C. Spatiotemporal variation of particulate fallout instances in Sfax City, southern Tunisia: influence of sources and meteorology. *Adv. Meteorol.* **2015**, *2015*, 471396. [[CrossRef](#)]
55. Fatma, O.M.A.; Murnira, O.; Nurul, B.A.W.; Latif, M. Compositions of dust fall around semi-urban areas in Malaysia. *Aerosol Air Qual. Res.* **2012**, *12*, 629–642.
56. Bisquert, D.S.; Castejón, J.M.P.; Fernández, G.G. The impact of atmospheric dust deposition and trace elements levels on the villages surrounding the former mining areas in a semi-arid environment (SE Spain). *Atmos. Environ.* **2017**, *152*, 256–269. [[CrossRef](#)]

-
57. Pan, G.; Li, S.L.; Zhu, L.; Sun, Y.M.; Zhang, G.Q. Study on Spatial and Temporal Distribution of Dust-fall Flux in Jinan City. *Ecol. Environ. Sci.* **2019**, *28*, 1802–1809.
 58. Li, S.Q.; Li, D.C.; Zhang, G.L. Atmospheric Dustfall Rates in Various Functional Zones of Nanjing and Its Influential Factors. *Soils* **2014**, *46*, 366–372.

Disclaimer/Publisher’s Note: The statements, opinions and data contained in all publications are solely those of the individual author(s) and contributor(s) and not of MDPI and/or the editor(s). MDPI and/or the editor(s) disclaim responsibility for any injury to people or property resulting from any ideas, methods, instructions or products referred to in the content.